A New Method to Investigate Denitrification Dynamics During Simulated Floods in Soils

Rana Kanaan, Romain Darnajoux, Laura Escarmena, Sabine Sauvage, Thierry Camboulive, Jean-louis Druilhe, José Miguel Sánchez-pérez

European Journal of Soil Science

WILEY

European Journal of Soil Science

METHODS ARTICLE OPEN ACCESS

A New Method to Investigate Denitrification Dynamics During Simulated Floods in Soils

Rana Kanaan[1] | Romain Darnajoux[1] | Laura Escarmena[2] | Sabine Sauvage[1] | Thierry Camboulive[1] | Jean-Louis Druilhe[1] | José Miguel Sánchez-Pérez[1]

[1]Centre de Recherche Sur la Biodiversité et l'Environnement, Université de Toulouse, CNRS, IRD, Toulouse INP, Toulouse, France | [2]Department of Evolutive Biology, Ecology and Environmental Sciences, University of Barcelona, Barcelona, Spain

Correspondence: Rana Kanaan (rana.kanaan@univ-tlse3.fr) | José Miguel Sánchez-Pérez (jose-miguel.sanchez-perez@univ-tlse3.fr)

Received: 3 December 2024 | **Revised:** 14 March 2025 | **Accepted:** 20 March 2025

Funding: This work was funded by the European Union through the ALFAWetlands project (H2020: HORIZON-CL5-2021-D1-01).

Keywords: laboratory experiment | nitrate pollution | nitrogen cycle | soil hydrology | wetlands

ABSTRACT

Riparian ecosystems, through their anoxic properties driven by floods, play a crucial role in favouring denitrification. The absence of nitrous oxide (N_2O) reductase activity in the denitrification process provokes the emission of a potent greenhouse gas (GHG), N_2O, into the atmosphere. Our understanding of the contribution of denitrification to N_2O emissions is limited by the difficulties in capturing peak N_2O events and measuring dinitrogen gas (N_2), the final product of the process under soil flooding. In this study, we describe the GHG-Aquacosme, a new laboratory-based and ecosystem-relevant approach to simulate flood conditions and investigate GHG flux dynamics in intact riparian soil cores, focusing on N_2O. The system capabilities were tested on two different riparian soils with simultaneous monitoring of N_2O, carbon dioxide and porewater chemistry. We also used a simple mass balance approach to estimate the N_2 emissions. The GHG-Aquacosme proved efficient in the incubation of soil samples under atmospheric conditions, preserving the initial soil structure and heterogeneity and providing a high temporal resolution of N_2O emission dynamics upon flooding. This translated into heterogeneous outputs in terms of N_2O dynamics and denitrification-related parameters such as N_2O yield and nitrate removal efficiency. Finally, accounting for nitrogen (N) species diffusion within the system is recommended, and the setup can easily accommodate isotopic N tracer methodologies to investigate other N cycle pathways. Further research is encouraged to determine how the results from the GHG-Aquacosme application can be utilised in predictive models of N_2O emissions, particularly in relation to future scenarios and projections of riparian flooding.

1 | Introduction

In riparian zones, the interface between land and adjacent aquatic ecosystems (Naiman et al. 2005) and stream-driven changes in the water table level contribute to a vital riparian function: biogeochemical cycling of elements, such as carbon (C) and nitrogen (N) (Gu et al. 2012). As one of the five major chemical elements on Earth, N is indispensable to life (Fowler et al. 2013). However, riparian wetlands are often sites of significant N loss that impact water quality, reduce nutrient availability and contribute to the emission of nitrous oxide (N_2O), a major stratospheric ozone-depleting substance and a greenhouse gas (GHG) with higher global warming potential than carbon dioxide (CO_2) and methane CH_4 (IPCC 2021). A variety of microbial processes contribute to N_2O emissions, including ammonium (NH_4^+) oxidation, co-denitrification, dissimilatory nitrate (NO_3^-) reduction to NH_4^+ (DNRA), coupled nitrification–denitrification, nitrifier denitrification and denitrification (Butterbach-Bahl

Summary

- The riparian zone is a hotspot of denitrification and N_2O emission that is complex to study.
- We present an experimental approach 'GHG-Aquacosme' to study the dynamics of N_2O emission and denitrification in riparian flooded soils.
- Intact soil cores were flooded and incubated under natural atmospheric conditions while GHGs were continuously monitored.
- Heterogeneous N_2O dynamics and denitrification patterns obtained from replicate soil cores.

et al. 2013; Harris et al. 2021; Hu et al. 2015; Masta et al. 2022; Wrage-Mönnig et al. 2018). Conversely, the microbial reduction of N_2O to N_2 is effectively catalysed by a single enzyme, N_2O reductase, found in both denitrifying and non-denitrifying microbes (Hallin et al. 2018). Denitrification, the stepwise reduction of NO_3^- to N_2 gas through the intermediates nitrite (NO_2^-), nitric oxide (NO) and N_2O (Jones et al. 2014), is a significant process in flooded riparian soils (Burgin and Groffman 2012).

The anaerobic conditions favoured by the waterlogging property of riparian zones during flooding initiate denitrification (Nishisaka et al. 2019), which requires not only the presence of NO_3^- as an electron acceptor, but also the availability of an electron donor, often as organic compounds (Butterbach-Bahl et al. 2013; Han et al. 2017) or inorganic compounds such as sulfide (Liu et al. 2016). The interplay between these fluctuating environmental variables and the microbiota carrying out denitrification leads to the emergence of complex spatio-temporal patterns of denitrification activity, which remain difficult to predict. A better understanding of the impact of environmental variables on the dynamics of denitrification and N_2O emissions is urgently required (Ansari et al. 2024; Vidon et al. 2018).

To understand the denitrification process, field (Audet et al. 2014; Fisher et al. 2014; Mafa-Attoye et al. 2020) and laboratory approaches (Burgin et al. 2010; Jacinthe and Vidon 2017; Petersen et al. 2020) rely mainly on quantifying the gaseous products, N_2 and N_2O, which allow the estimation of N_2O yield (Bizimana et al. 2022; Wang et al. 2020).

In general, laboratory studies, compared to field-based studies, can better control environmental variables known to influence denitrification (Li et al. 2023; Maag et al. 1997; Woodward et al. 2009); they yield results that are less representative of ecosystem processes. In addition, the choice of methodology can also influence denitrification estimates. In saturated riparian soils, denitrification studies often face a common set of limitations: disruption of the soil's physical structure, use of artificial atmospheric conditions during incubation and low temporal resolution. For example, while the slurry incubation technique is commonly used to study denitrification from saturated riparian soils (Groh et al. 2019), it can overestimate or underestimate the process as it includes soil aggregate destruction and elimination of the physical structure's impact on denitrification (Vidon and Hill 2004). Indeed, the destruction and repacking of soil cores can modify denitrification outcomes (Balaine et al. 2013). Addy et al. (2002) described an in situ push-pull method that provided lower denitrification rates in saturated riparian locations than those previously observed in the field. A similar push-pull method approach was used to study denitrification in saturated riparian wetlands by integrating acetylene amendments (Sánchez-Pérez et al. 2003). The latter application is limited because of the problematic interference of acetylene with C degradation, nitrification pathway (Davidson and Seitzinger 2006), and catalytic decomposition of NO (Nadeem et al. 2013).

N_2-free atmospheric incubation, such as helium (He), has also been used in denitrification studies of intact riparian soil cores (Mander et al. 2014); however, this procedure is constrained by sophisticated tight incubations and the time required to establish an N_2-free atmosphere in the soil core (Butterbach-Bahl et al. 2013). ^{15}N-tracing approach (Masta et al. 2022) is another laboratory technique that is also applicable in riparian saturated soil studies (Ye et al. 2023) to trace labelled denitrification products; however, it requires exogenous and homogeneous amendments of ^{15}N-labelled NO_3^-.

Although these approaches are useful for studying denitrification, a high-sensitivity method that studies N_2O and denitrification dynamics in an environmentally relevant setup with high temporal resolution is still needed (Vidon et al. 2015; Zhang et al. 2023). The reported temporal resolution of N_2O emissions and denitrification at riparian sites is often seasonal (Hefting et al. 2006) or monthly (Ensign et al. 2008), which could underestimate hot moments and hotspot occurrences upon flooding.

Here, we report on a high temporal resolution system, 'GHG-Aquacosme' that allows the simulation of floods in intact soil cores under free-air incubation with continuous monitoring of N_2O and CO_2 emissions, soil moisture and temperature conditions. The proposed system allows (a) characterisation of N_2O emission dynamics, (b) measurement of short-term changes in several soil physiochemical characteristics, such as NO_3^-, NO_2^- and NH_4^+, and (c) estimation of N_2O yield via a mass balance approach. The GHG-Aquacosme system was tested in two different riparian soils, with or without NO_3^- amendments.

2 | Material and Methods

2.1 | Theoretical Framework

To characterise the spatial and temporal heterogeneity of N_2O emissions upon riparian wetland flooding, we defined three variables: t_{max}, N_2O_{max} and $N_2O_{quantity}$ (Figure 1A). t_{max} is the time required to reach the maximum N_2O emissions. N_2O_{max} is the maximum emission of N_2O reached, while $N_2O_{quantity}$ is the total quantity of N_2O emitted under flooded conditions.

The removal of NO_3^- occurred through denitrification and produced $N_2O_{(g)}$ and $N_{2(g)}$. Knowing that NO_3^- can be reduced via DNRA to NH_4^+, we assumed that when NH_4^+ and NO_2^- represent a minor fraction of the initial NO_3^- ($\leq$15%) and when there is no evidence of NO_3^- production, the NO_3^- lost by the system and not

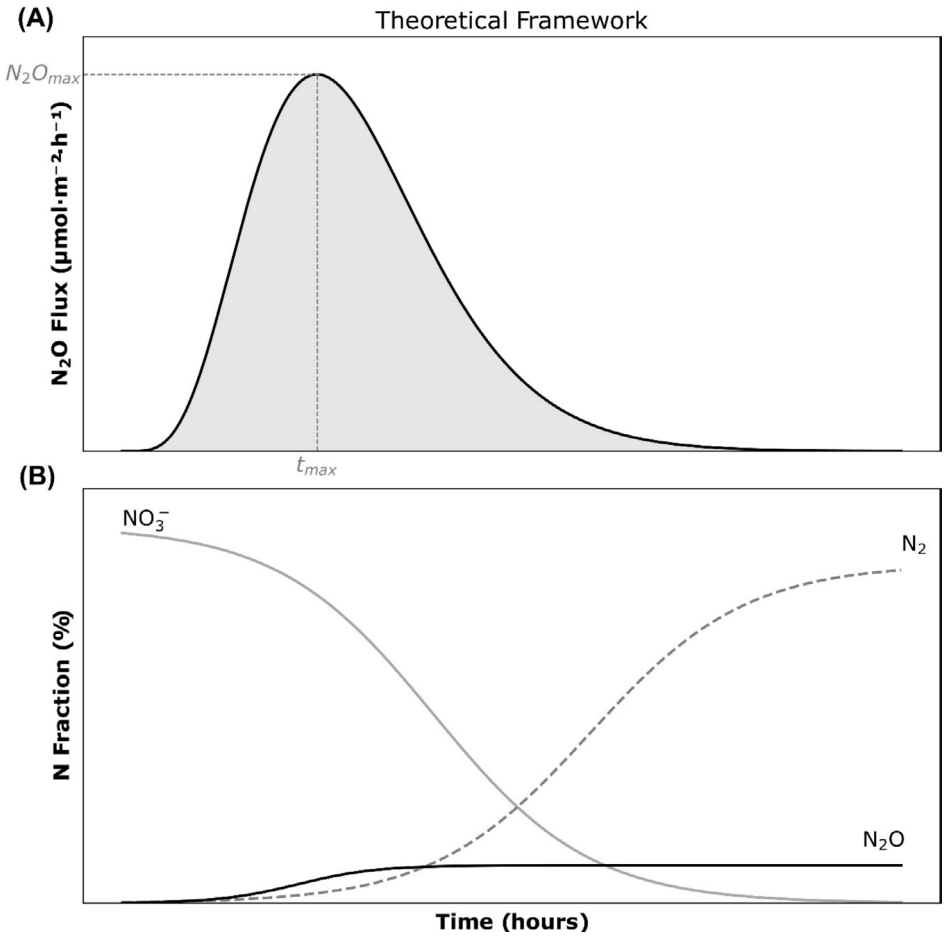

FIGURE 1 | Theoretical framework of GHG-Aquacosme. (A) Schematic representation of N_2O dynamic characteristics: t_{max}, N_2O_{max} and $N_2O_{quantity}$ (grey shaded area under the N_2O curve), and (B) theoretical evolution of the N fractions (NO_3^-, N_2O and N_2) during the flood-induced denitrification event under open atmosphere incubation. NO and NO_2^- are not represented.

accounted for by the N_2O produced provides a reliable estimate of the N_2 emitted during the same period (Figure 1B; Equation 1).

$$\text{Estimated } N_2 = \Delta NO_3 - N_2O \quad (1)$$

During water-saturated conditions and between the two time points, Estimated N_2 = estimated N_2 quantity (µmol) produced. N_2O = measured N_2O quantity (µmol) produced. ΔNO_3 = Measured difference in NO_3^- quantity (µmol).

Under these assumptions, the ratio of N_2O produced to NO_3^- removed (R_{N_2O}) is a proxy for N_2O yield. Finally, the ratio of the total NO_3^- removed to the initial NO_3^- provides an estimate of the NO_3^- removal efficiency via denitrification (%Denitrification) in the tested soils.

2.2 | GHG-Aquacosme

2.2.1 | System Design

The GHG-Aquacosme (Figure 2A) is a laboratory-based approach that enables the incubation of intact soil cores under preferred environmental conditions. It is composed of four waterproof glass aquariums (length × height × width = 80 × 40 × 30 cm). Each aquarium has three polyvinyl chloride (PVC) cylinders (height × diameter = 20 × 12.5 cm) that hold the soil core. The cylinder, with a perforated base and open surface (Figure 2B) is connected to plexiglass gas collection chambers (height × diameter = 20 × 12.5 cm), a PVC cap equipped with four leak-proof connectors and an air pump (ventilation system). During the experiment, the soil cores alternate between the open and enclosed incubation phases through the automatic control of electronic valves connected to a logic controller. During the open incubation phase, the soil core is exposed to atmospheric conditions by using a ventilation system. In contrast, during the enclosed incubation phase, which blocks the ventilation system, GHGs accumulate within the gas collection chamber, enabling the estimation of the GHG fluxes. A technical description of the GHG-Aquacosme design, control and programming is provided in the Supporting Information.

Each aquarium is connected to a water pump with four inlets and four outlets, allowing addition or removal of water at the base. By progressively adding water to the aquarium's base, it infiltrates the soil core through the perforated sheet in an upward direction, similar to a water table whose height can be controlled.

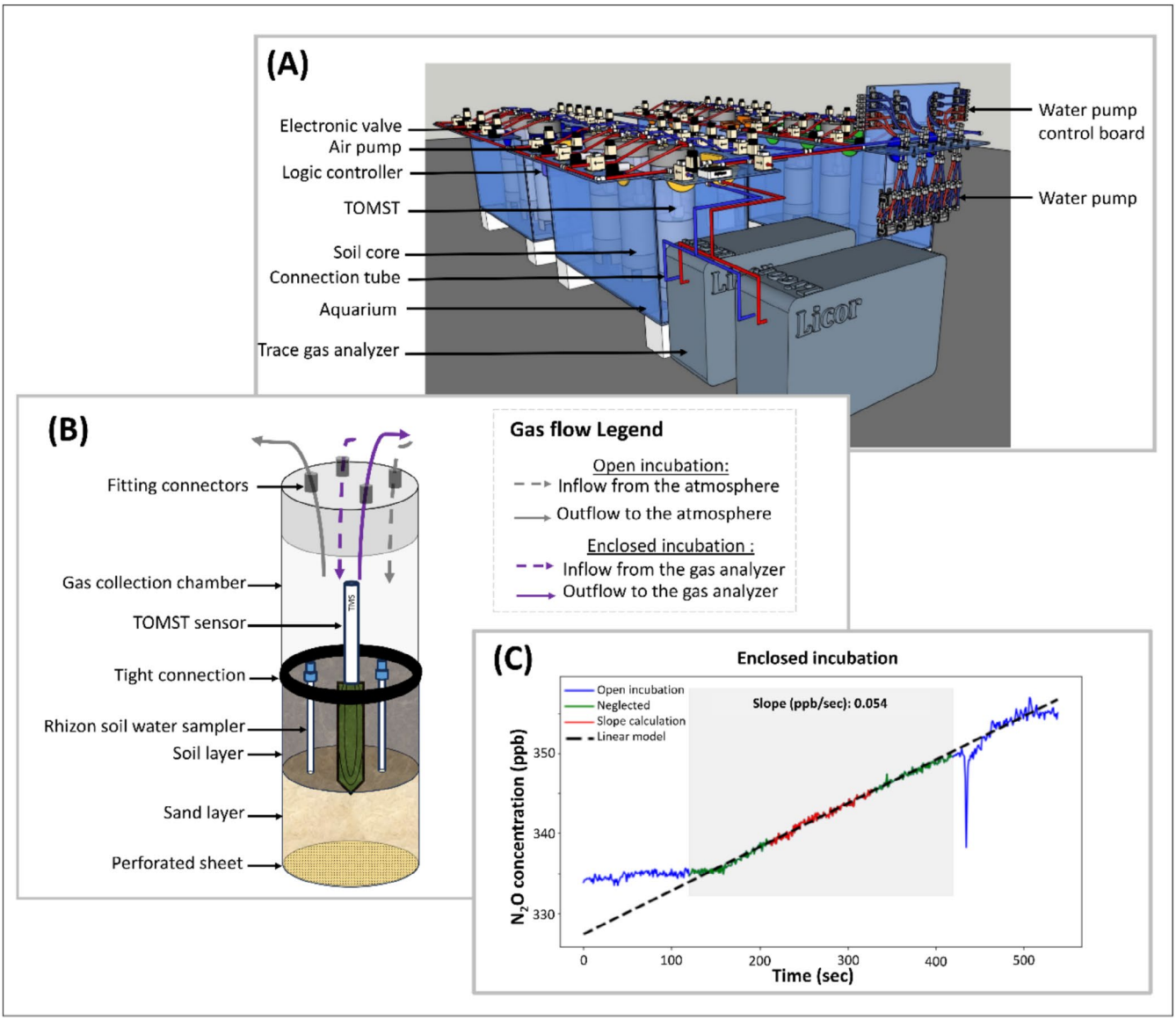

FIGURE 2 | (A) GHG-Aquacosme system design, (B) soil core design and (C) evolution of N_2O concentration and linear regression obtained during typical incubation.

2.2.2 | GHG Monitoring

To continuously monitor the concentrations of N_2O, CO_2 and CH_4 during the GHG-Aquacosme operation, two commercially available laser-based optical feedback cavity enhanced absorption spectroscopy (OF-CEAS) gas analysers were connected to the GHG-Aquacosme: LI-COR LI-8100/A N_2O/H_2O and LI-7810 $CH_4/CO_2/H_2O$ Trace gas analysers (https://www.licor.com/). The measurement ranges for N_2O, CH_4 and CO_2 were 0–100, 0–100 and 0–10,000 ppm, respectively. The precision (1σ) determined through repeated measurements for LI-8100/A N_2O/H_2O was 0.40 ppb at 330 ppb with 1 s averaging and 0.20 ppb at 330 ppb with 5 s averaging. As we assume that the dissolved N_2O will ultimately be either released to the atmosphere and measured or reduced to N_2, we focused on measuring the N_2O flux to the atmosphere.

2.2.3 | Environmental Variables Monitoring

TMS-3 dataloggers (TOMST; Figure 2B) are used to continuously monitor the volumetric moisture (time-domain transmission principle) and soil temperature inside the soil core (Wild et al. 2019). The atmospheric pressure and temperature of the GHG-Aquacosme during the experiment are recorded using an external pressure and temperature sensor (HP206C).

To follow the evolution of chemical properties in the incubated soil cores, replicate soil porewater samples were obtained simultaneously using two permanently installed MacroRhizons water samplers (Rhizosphere Research Products, length: 10 cm, average pore size: 0.15 μm) (Seeberg-Elverfeldt et al. 2005) (Figure 2B). The two extracted porewater samples are

mixed to obtain a homogenised water sample. These samples are then stored at 4°C until further analysis in the PAPC facility at University Paul Sabatier (https://chemicalanalysis.cnrs.fr/) using standardised protocols. The main analytes in porewater are N species (NO_3^-, NO_2^-, NH_4^+), control species chloride (Cl^-), potassium (K^+) and Phosphate (PO_4^{3-}), Total dissolved Nitrogen (TN), dissolved organic carbon (DOC) and organic acids. More information on the water sample analyses is summarised in Table S1.

2.2.4 | N_2O Flux Calculation

After retrieving the GHG concentration data from the trace gas analysers, the GHG production rates (S) are calculated for each core and time period using least-squares linear regression over the linear part of the measurement (Figure 2C). We excluded the initial and final 90 s from the 5-min measurement duration to account for the stabilisation and oversaturation phases at the start and end of the enclosed incubation phases, respectively. The GHG Fluxes were then calculated using Equation (2).

$$\text{GHG Flux} = \frac{\left(\frac{P \times V}{R \times T \times A}\right) \times S}{1000} \quad (2)$$

where GHG Flux (expressed in μmol m^2 h^{-1} and μmol m^2 s^{-1} for N_2O and CO_2, respectively). P = Pressure (Pa). V = Total volume of gas collection chamber and connecting tubes to the gas analysers (m^3). R = Universal gas constant (8.314 J mol^{-1} K^{-1}). T = Temperature (K). A = surface area of the core (m^2). S = GHG production rates (in ppb s^{-1} for N_2O and ppm s^{-1} for CO_2).

The total quantity of each GHGs emitted was calculated using the trapezoidal rule for numerical integration applied between two consecutive measurements (2 h), and the results summed over the duration of the experiments. All calculations were done using Python software (v.3.11) and Spyder (v.5.4.3).

3 | GHG-Aquacosme Experimental Validation

3.1 | Study Sites and Soil Sampling

To test the efficiency of the GHG-Aquacosme, we chose two riparian forest sites: Site I and Site II. Site I is located in the Cànoves i Samalús forest in Catalonia, Spain, which regularly receives treated effluent from a wastewater treatment plant via a shunt (Escarmena et al. 2024). Site I soil was characterised by a sandy loam texture, with a total N content averaging 0.2% ± 0.03% and organic C content averaging 2.48% ± 0.71%. Site II is located at the confluence of the Garonne and Ariège Rivers in Toulouse, France, and experiences annual natural flooding. The soils from Site II exhibited a silty loam texture, with a total N content averaging 0.34% ± 0.07% and organic C content averaging 4.84% ± 1.38%. At each studied site, three intact undisturbed soil cores were taken 3 m apart under natural soil moisture. The soil cores were carefully extracted from the uppermost 10 cm of the soil layer using a metallic corer with dimensions matching those of the soil core (10 cm in length, 12.5 cm in diameter), and subsequently transferred to PVC cylinders previously half-filled (10 cm) with sand.

3.2 | Experimental Setup

The soil cores were brought to the lab, where a TOMST sensor and two porewater samplers were permanently inserted in the middle of each intact soil core (Figure 2B). GHG-Aquacosme validation consisted of two sequential experiments conducted at room temperature: an initial experiment (Experiment 1) simulating flooding through a rise in the water table level, followed by a second experiment (Experiment 2) assessing the riparian soil NO_3^- buffering capacity through addition of NO_3^- at varying concentrations.

In Experiment 1, flooding was simulated in the three soil cores (S1, S2 and S3) via the addition of distilled water through water pumps to the aquarium base. Accordingly, water infiltrates the soil core from the bottom and rises within it. When the water table inside the soil cores reaches the upper soil surface, the water addition to the aquarium is stopped, which represents the start of Experiment 1. The flood duration and continuous N_2O monitoring lasted 142 h after flood initiation. Simultaneously, paired porewater samples were extracted from each soil core at 0, 49, 93 and 141 h during the flood phase. In Experiment 2, the three flooded soil cores were injected with KNO_3 at multiple locations and depths using a 12 cm needle to reach three theoretical NO_3^- concentrations (C1 = 110, C2 = 220 or C3 = 440 mg L^{-1}). Following the addition of NO_3^-, the N_2O levels were continuously measured for another 160 h. Simultaneously, paired porewater samples were extracted at 24, 72, 96 and 160 h. No samples were extracted in the first 24 h to prevent excessive removal of the recently introduced NO_3^-. The extracted paired soil porewater samples were homogenised and assessed for their chemical properties according to the GHG-Aquacosme environmental variable monitoring protocol (see Section 2.2.3).

4 | Results

We evaluated the operational capability of the system by following the evolution of GHG fluxes (N_2O and CO_2), NO_3^-, control species, soil moisture and soil temperature from Site I soils before and after NO_3^- supplementation (Figure 3). The results from Site II are shown in SI (Figure S1). The variations in CH_4, NO_2^- and NH_4^+ are shown in Figures S2 and S3. The overall dynamic characteristics of N_2O emissions, including total $N_2O_{quantity}$, t_{max} and N_2O_{max}, N_2O:CO_2 ratio and initial NO_3^- concentration, are presented in Table 1 for Sites I and II soil cores. Denitrification-related parameters such as R_{N_2O} and %Denitrification are shown in Table 2.

4.1 | System Stability

During the flood simulation before NO_3^- amendment, the moisture content integrated over the first 10 cm increased rapidly in all three replicate samples from under 80% to 100% within

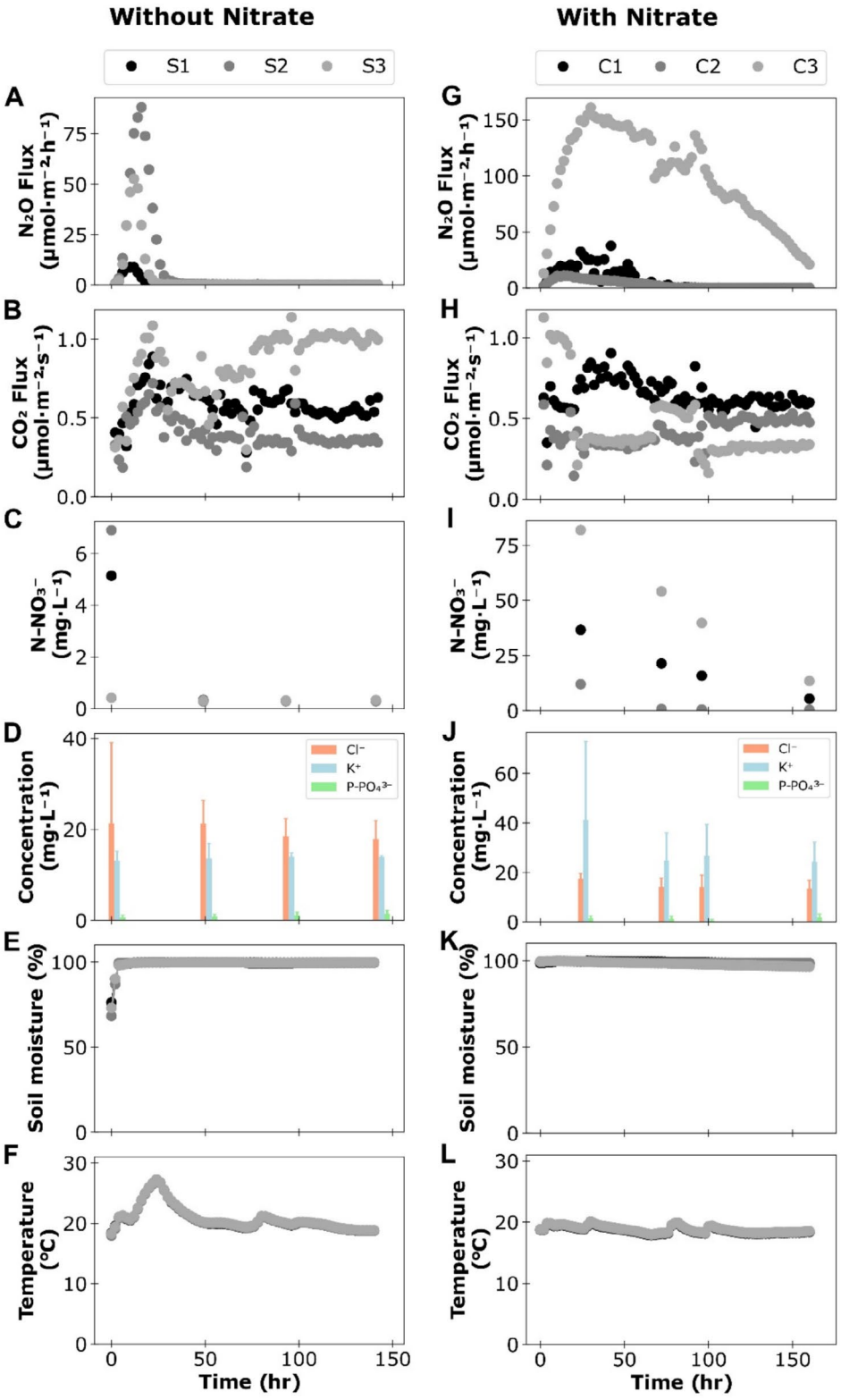

FIGURE 3 | Evolution of GHG fluxes (N_2O, CO_2), porewater NO_3^-, control species (Cl^-, K^+ and PO_4^{3}), soil moisture and soil temperature during flood simulation at Site I. The left panel shows the results from triplicate soil cores without NO_3^- amendments (S1, S2 and S3), and the right panel shows the results from soil cores after variable NO_3^- amendments (C1 = 110, C2 = 220 and C3 = 440 mg L^{-1}).

a 4-h period. Subsequently, it was maintained at a level of approximately 99% or higher throughout the incubation process (Figure 3E). After NO_3^- amendment, the moisture content experienced a minor reduction but remained consistently above 96.5% (Figure 3K).

The temperature was maintained at approximately 20°C before and after the NO_3^- addition (Figure 3F,L). At the beginning of Experiment 1 (10–30 h), the soil temperature experienced large fluctuations in amplitude (19°C–26°C) during the setup of the heating probes before stabilisation (Figure 3F).

TABLE 1 | N_2O dynamic characteristics, N_2O to CO_2 ratios and initial NO_3^- concentrations in Sites I and II before (S1, S2 and S3) and after NO_3^- amendment (C1 = 110, C2 = 220, and C3 = 440 mg L^{-1}).

Site	Flood condition	Sample	Total $N_2O_{quantity}$ μmol	t_{max} h	N_2O_{max} μmol m^{-2} h^{-1}	N_2O:CO_2 [ppb:ppm]	Initial NO_3^- mg_N L^{-1}
Site I	Without nitrate	S1	1.1	10.0	9	0.34	5.14
		S2	12.2	16.0	88	5.67	6.91
		S3	5.2	12.0	53	1.14	0.41
		Mean	6.2	12.7	50	2.38	4.15
		SD	4.6	2.5	33	2.35	2.74
	With nitrate	C1	11.5	42.0	38	2.91	25*
		C2	5.1	14.0	11	2.04	50*
		C3	169.8	30.0	161	65.33	100*
		Mean	62.1	28.7	70	23.42	58.33*
		SD	76.2	11.5	65	29.63	31.18*
Site II	Without nitrate	S1	13.2	8.0	147	1.18	13.00
		S2	0.2	4.0	3	0.04	3.19
		S3	0.1	2.0	0	0.02	0.71
		Mean	4.5	4.7	50	0.41	5.64
		SD	6.1	2.5	69	0.54	5.31
	With nitrate	C1	5.3	16.0	33	0.88	25*
		C2	4.2	18.0	19	1.12	50*
		C3	21.1	30.0	43	6.03	100*
		Mean	10.2	21.3	32	2.67	58.33*
		SD	7.7	6.2	10	2.37	31.18*

*Corresponds to unmeasured theoretical N-NO_3^- concentrations immediately after NO_3^- amendment.

TABLE 2 | Assessment of denitrification-related parameters under naturally occurring nitrate conditions.

Site	Sample	R_{N_2O} %	%Denitrification %
Site I	S1	1.2	94
	S2	9.0	96
	S3*	66.0	20
	Mean	25.4	70
	SD	28.9	35
Site II	S1	4.5	96
	S2*	0.2	79
	S3*	0.3	42
	Mean	1.7	72
	SD	2.0	23

*Corresponds to the sample where mass balance is less accurate due to the evidence of NO_3^- production.

The hydrological stability of the system was evaluated by monitoring Cl^- and PO_4^{3-} concentrations, which remained steady during incubation before and after NO_3^- addition (Figure 3D,J). While K^+ concentrations were constant before NO_3^- addition, they increased after NO_3^- amendment (Figure 3J) and then decreased and stabilised after 72 h.

4.2 | Dynamics of GHG Fluxes

While N_2O flux exhibited a distinct dynamic evolution (Figure 3A,G) during flood simulation, CO_2 fluxes exhibited a less consistent pattern and did not follow the same dynamics during flood simulation before (Figure 3B) or after (Figure 3H) NO_3^- amendments in Site I. Prior to NO_3^- additions, soil replicates from the two sites showed comparable mean total N_2O quantities in μmol (6.2 ± 4.6 and 4.5 ± 6.2 μmol for Site I and Site II, respectively) but with very large variability (expressed as SD). The mean t_{max} in Site I soils (12.7 ± 2.5 h) was higher than that in Site II soils (4.7 ± 2.5 h). Similar maximal N_2O fluxes (N_2O_{max}) were observed across the two sites (50 ± 33 and

$50 \pm 69\,\mu mol\,m^{-2}\,h.^{-1}$, for Site I and Site II soils, respectively). The mean N_2O:CO_2 ratio in ppb:ppm varied from 2.38 ± 2.35 in Site I to 0.41 ± 0.54 in Site II soils.

After NO_3^- addition, the soil cores treated with the highest concentration of NO_3^- (C3) demonstrated the greatest N_2O quantity and N_2O_{max} compared to the C1 and C2 samples. This trend was observed in both Site I (169.8 µmol and 161.0 $\mu mol\,m^{-2}\,h^{-1}$) and Site II (21.1 µmol and 43.0 $\mu mol\,m^{-2}\,h^{-1}$) soil cores.

4.3 | N-Species (NO_3^-, NO_2^- and NH_4^+) Evolution

At the beginning of the flood simulation, the mean porewater NO_3^- concentration was 4.15 ± 2.74 $mg_N\,L,^{-1}$ which was nearly depleted after 40 h of flood simulation. Following NO_3^- amendments, pooled soil porewater from the two porewater samplers showed a steady decline in NO_3^- concentration over time (Figure 3I), with the lowest concentrations (6.43 ± 5.37 $mg_N\,L^{-1}$) reached after 160 h of incubation. NO_2^- remained low and stable at concentrations below 2 $mg\,L^{-1}$ (Figure S2). NH_4^+ remained undetectable (below 0.003 $mg_N\,L^{-1}$) before NO_3^- additions and increased slightly in concentration, reaching 0.67 ± 0.37 $mg_N\,L^{-1}$ by the end of the NO_3^- incubation phase (Figure S2).

4.4 | Denitrification

We assessed denitrification parameters in the flooding experiment with natural nitrate (Experiment 1). R_{N_2O} exhibited a higher mean (25.4%) in Site I than in Site II soils (1.7%) (Table 2), whereas both showed high variability (SD = 28.9% and 2.0% in Site I and Site II soils, respectively). The two soil types showed a similar %Denitrification ($70\% \pm 35\%$ and $72\% \pm 23\%$).

Finally, we used the mass balance approach (Equation 1) between the measured time points (0, 49, 93 and 141 h) in the experiments showing no evidence of NO_3^- production (see Figure 4) to track how the added N present in the system is transformed over time into its various species. N_2O measured by the system represents only a fraction of the NO_3^- lost (less than 10%). As the other N species measured in the porewater over time (NH_4^+ and NO_2^-) remained low ($\leq 15\%$ of initial NO_3^-) and the experimental conditions favoured denitrification, we accounted for the missing N as N_2 gas (see Figure 4, dotted line). N_2O production slowed over time and remained mostly constant after 60 h, whereas NO_3^- was still removed from the systems, leading to a decrease in cumulative N_2O production over time (see Figure 4C).

5 | Discussion

5.1 | Performance of the System

In this study, we provided a new methodology to better understand denitrification in riparian soil samples. Our system was able to generate an ecosystem-relevant N_2O flux dynamic (Figure 3A,G) and to provide insights into the denitrification process by following the evolution of porewater chemistry, as well as by estimating characteristic parameters such as R_{N_2O}, N_2O:CO_2, and %Denitrification (Figure 4, Tables 1 and 2).

First, our system simulates the upward movement of groundwater, resembling one of the riparian flooding scenarios. Moisture levels integrated over the first 10 cm increased rapidly to nearly 100% moisture within 4 h and with a mean of $99\% \pm 0.6\%$ across replicates throughout the incubation period, promoting anaerobic conditions required for denitrification and N_2O emission. Secondly, after an initial fluctuating period due to the setup of the heating system (between 10 and 30 h before NO_3^- addition), temperature remained stable at approximately 20°C ($19.9°C \pm 1.0°C$), providing a consistent condition for microbial activity and denitrification. Minimal changes in Cl^- and PO_4^{3-} concentrations before and after NO_3^- addition indicate the hydrological stability of the GHG-Aquacosme system. Conversely, K^+ concentrations increased immediately following NO_3^- amendments, likely due to KNO_3 being the NO_3^- source, raising the K^+ concentration.

Automated N_2O measurement, performed every 2 h, enabled the study of N_2O dynamics over several days with excellent time resolution (Figure 3A,G). The range of t_{max} obtained in our experiment (Table 1) is in line with denitrification enzyme kinetics and the de novo synthesis of nitrous oxide after 24–42 h of anaerobic incubation (Zheng and Doskey 2015). The evolved bell-shaped dynamics of N_2O in GHG-Aquacosme were similar to the patterns obtained in anaerobic incubation of agricultural soil cores, which exhibited an N_2O peak either at 24 h (Wang et al. 2011) or with a delay of 1–2 days (Bergstermann et al. 2011; Castellano-Hinojosa et al. 2019; Loick et al. 2017). Through NO_3^- amendments, the system demonstrated its ability to evaluate the environmental balance between the buffer capacity of riparian zones and GHG emissions (Hefting et al. 2003; Walton et al. 2020; Welsh et al. 2021).

The GHG-Aquacosme system also enabled us to simultaneously monitor CO_2 and CH_4 fluxes (Figure 3B,H, Figures S2 and S3), and thus to investigate patterns of co-occurrence between the processes. The N_2O:CO_2 ratios (Table 1), which are highly variable and difficult to interpret, can help investigate the link between denitrification and carbon cycling processes under environmentally relevant conditions. The GHG-Aquacosme allowed us to capture the heterogeneous GHG dynamics (t_{max}, N_2O_{max} and $N_2O_{quantity}$) between replicate samples from the same site (Table 1). Unlike other methods that use sieved and artificially compacted soils to study denitrification (Castellano-Hinojosa et al. 2019; Loick et al. 2017), the minimally disturbed soil cores in our method consider the impact of natural soil structure and spatial heterogeneity on denitrification processes and N_2O emissions. When using repacked soil cores, Balaine et al. (2013) found that while peak N_2O emissions occurred at a given value of water-filled pore space, this value varied markedly across a range of soil bulk densities. Thus, artificially repacking the soil can modify the results of denitrification experiments.

Intact soil core incubation to monitor N_2O emissions has already been proposed with different setups, such as that proposed by Button et al. (2023) to address field-relevant N_2O emissions. Compared with other setups (Burgin et al. 2010; Butterbach-Bahl et al. 2002), GHG-aquacosme-incubated soils were under

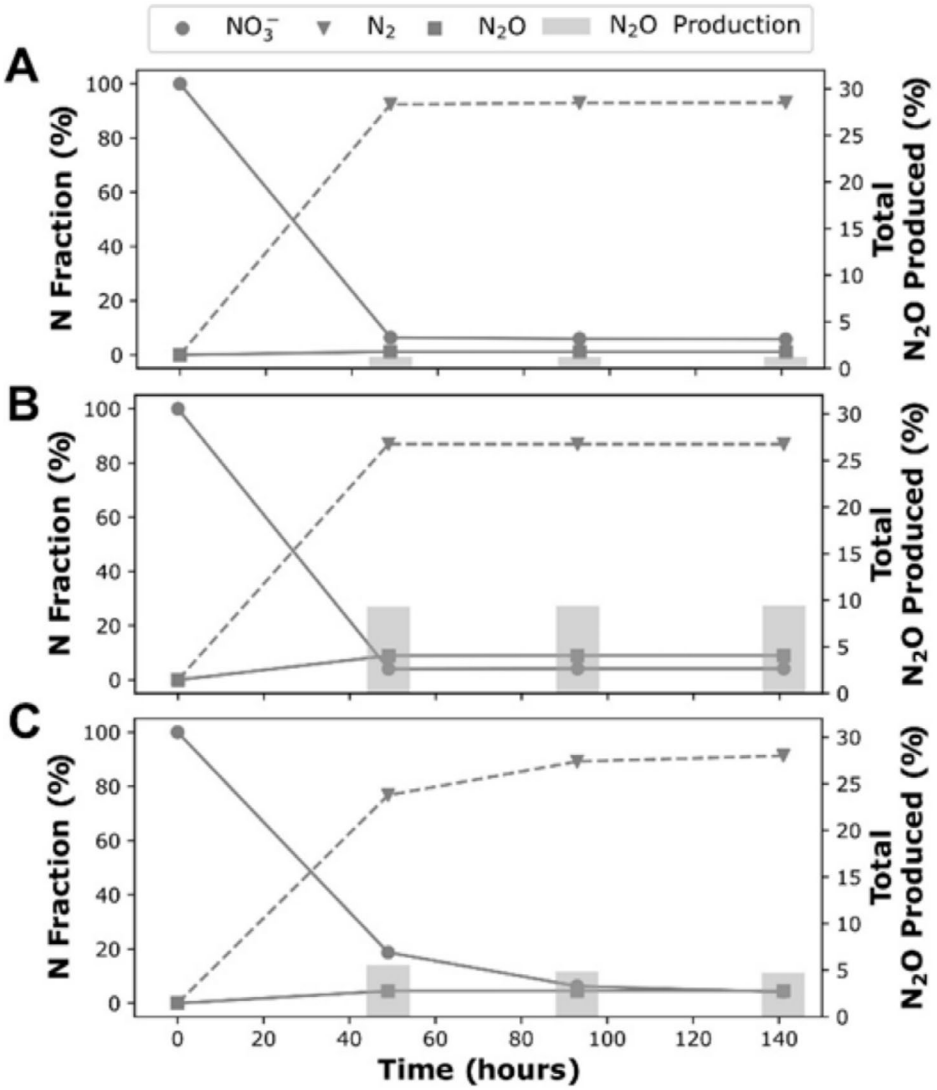

FIGURE 4 | The evolution of the natural N pool between the different N species was expressed as the percentage of initial NO_3^- in the porewater from Site I (A and B) and Site II (C) riparian soil samples. Porewater NO_3^- (circle) and N_2O (square) were directly measured, while N_2 (dotted line, triangle) was estimated using the mass balance according to Equation (1). Solid grey bars (secondary *y*-axis) represent the total fraction of N lost as N_2O over time (R_{N_2O}).

natural atmospheric conditions rather than an artificial He atmosphere. While other methods used intact soil cores and open systems (Button et al. 2023; Kemmann et al. 2023), they usually lack the temporal resolution of the GHG-Aquacosme. Similarly, the GHG-Aquacosme system demonstrated enhanced temporal resolution of the dynamics of GHG when compared to the setup of Wang et al. (2019), which created artificial floods in undisturbed soil samples from freshwater and saltwater marshes under atmospheric conditions and utilised automated GHG measurements with a minimal of 24h.

5.2 | Limitations and Recommendations

Despite aiming to replicate field conditions in the GHG-Aquacosme, several limitations persist. The flooding scenario was initially set up to progress from the bottom upward in the soil core; however, the water flow system of GHG-Aquacosme is handy enough to be adjusted to simulate floods in the reverse direction. This modification would account for both the potential flooding patterns observed in riparian wetlands: upward water table movement and stream flooding. The soil core design, which permits direct bottom-water contact, does not reproduce the soil depth gradient and likely allows oxygen diffusion from the surrounding water, creating a double gradient rather than a steady vertical gradient. To mitigate this, a sand layer was incorporated into the bottom of the soil core. Furthermore, we noticed that in highly active soil cores, the air exchange rate could not fully replace the produced N_2O gas in the headspace. This could be resolved by increasing the air flux, but this could lead to a decrease in the vessel inner pressure and an increase in the water level in the soil core. This issue can be resolved by adapting the diameter of the output tubing.

To limit the exchange of N species between the soil core and aquarium water, we added 10 cm of sand at the bottom of each core. However, it is likely that some NO_3^- was lost through diffusion in the aquarium, leading to a bias in the mass balance

and underestimation of the denitrification parameters. To address this issue further, we recommend that (1) simultaneously measure the chemical properties of water both within the soil core and in the surrounding water in the aquarium to evaluate the potential for diffusion, (2) separate the soil cores in mini-aquariums and (3) provide NO_3^- directly through the aquarium water, rather than needle injection, to decrease the concentration gradient and obtain a more uniform distribution of NO_3^- within the soil core. Additionally, the use of a tracer ion, such as Br^- or Cl^-, can help correct N species diffusion outside the soil core.

In our demonstration, two soil porewater samples were extracted and mixed to represent the overall chemistry of the soil core. While the 10 cm porewater sampler should integrate the water chemistry across 10 cm of the soil core, it is important to highlight that the mean value we obtained might be biased due to lateral spatial heterogeneity in the porewater chemistry. We recommend analysing the two porewater samples separately to estimate heterogeneity due to the presence of active hotspots.

Finally, N_2 production and N_2O yield estimates using GHG-Aquacosme may be biased by neglecting the entrapped gas, loss of N as NO, amount of N_2O dissolved in the water and other N pathways (e.g., DNRA). In cases where no evidence of NO_3^- production and other N species represent a small fraction (< 15% of initial NO_3^-), we found that R_{N_2O} represents less than 10% of total NO_3^- loss, aligned with literature estimates (Denmead et al. 1979; Lind et al. 2013). However, when NO_3^- is low, other N species tend to be more important and only N_2O emissions can be accurately quantified. To solve this, our system can be used in conjunction with ^{15}N isotopic labelling methodologies to further elucidate more complex N dynamics under realistic water table conditions and background NO_3^- concentrations.

6 | Conclusion and Perspectives

This study aimed to describe and evaluate a new mesocosm application, the GHG-Aquacosme. This system allowed for the characterisation of N_2O flux dynamics and quantity in intact soil cores from contrasted riparian sites through continuous N_2O monitoring under simulated flood conditions. The GHG-Aquacosme incubates soil under atmospheric conditions, effectively mimicking floods while preserving the soil structure, thereby revealing ecosystem-relevant heterogeneous N_2O fluxes. The setup reproduces expected N_2O production patterns and enables the identification of denitrification-related parameters, such as NO_3^- removal efficiency and N_2 estimation based on the mass balance approach. The initial assessment of the capacity of the GHG-Aquacosme allows us to delimit the possibilities of the methods and recommendations to further improve its range of applications, such as the integration of isotopic tracing techniques.

Overall, the GHG-Aquacosme can produce high temporal resolution data on N_2O emissions at the hourly scale, which helps in the development of denitrification models and in predicting N_2O emissions upon future flooding projections in riparian wetlands.

Author Contributions

Rana Kanaan: writing – original draft, formal analysis, methodology, visualization, investigation. **Romain Darnajoux:** writing – review and editing, formal analysis, supervision, methodology, visualization. **Laura Escarmena:** methodology, visualization, formal analysis, investigation. **Sabine Sauvage:** writing – review and editing, methodology, conceptualization, supervision, funding acquisition. **Thierry Camboulive:** methodology. **Jean-Louis Druilhe:** methodology, software. **José Miguel Sánchez-Pérez:** conceptualization, methodology, writing – review and editing, project administration, funding acquisition, supervision.

Acknowledgements

This project received funding from ALFAwetlands projects. We thank the support received from the University of Toulouse. For the support during the field and lab work, we thank Noémie Carles.

Conflicts of Interest

The authors declare no conflicts of interest.

Data Availability Statement

The data that support the findings of this study are available from the corresponding author upon reasonable request.

References

Addy, K., D. Q. Kellogg, A. J. Gold, P. M. Groffman, G. Ferendo, and C. Sawyer. 2002. "In Situ Push–Pull Method to Determine Ground Water Denitrification in Riparian Zones." *Journal of Environmental Quality* 31, no. 3: 1017–1024. https://doi.org/10.2134/jeq2002.1017.

Ansari, J., S. Bardhan, M. P. Davis, S. H. Anderson, and N. Al-Awwal. 2024. "Greenhouse Gas Emissions From Riparian Systems as Affected by Hydrological Extremes: A Mini-Review." *Cogent Food & Agriculture* 10, no. 1: 2321658. https://doi.org/10.1080/23311932.2024.2321658.

Audet, J., C. C. Hoffmann, P. M. Andersen, et al. 2014. "Nitrous Oxide Fluxes in Undisturbed Riparian Wetlands Located in Agricultural Catchments: Emission, Uptake and Controlling Factors." *Soil Biology and Biochemistry* 68: 291–299. https://doi.org/10.1016/j.soilbio.2013.10.011.

Balaine, N., T. J. Clough, M. H. Beare, S. M. Thomas, E. D. Meenken, and J. G. Ross. 2013. "Changes in Relative Gas Diffusivity Explain Soil Nitrous Oxide Flux Dynamics." *Soil Science Society of America Journal* 77, no. 5: 1496–1505. https://doi.org/10.2136/sssaj2013.04.0141.

Bergstermann, A., L. Cárdenas, R. Bol, et al. 2011. "Effect of Antecedent Soil Moisture Conditions on Emissions and Isotopologue Distribution of N_2O During Denitrification." *Soil Biology and Biochemistry* 43, no. 2: 240–250. https://doi.org/10.1016/j.soilbio.2010.10.003.

Bizimana, F., J. Luo, A. Timilsina, et al. 2022. "Estimating Field N_2 Emissions Based on Laboratory-Quantified $N_2O/(N_2O + N_2)$ Ratios and Field-Quantified N_2O Emissions." *Journal of Soils and Sediments* 22, no. 8: 2196–2208. https://doi.org/10.1007/s11368-022-03212-0.

Burgin, A. J., and P. M. Groffman. 2012. "Soil O_2 Controls Denitrification Rates and N_2O Yield in a Riparian Wetland." *Journal of Geophysical Research: Biogeosciences* 117, no. G1: 2011JG001799. https://doi.org/10.1029/2011JG001799.

Burgin, A. J., P. M. Groffman, and D. N. Lewis. 2010. "Factors Regulating Denitrification in a Riparian Wetland." *Soil Science Society of America Journal* 74, no. 5: 1826–1833. https://doi.org/10.2136/sssaj2009.0463.

Butterbach-Bahl, K., E. M. Baggs, M. Dannenmann, R. Kiese, and S. Zechmeister-Boltenstern. 2013. "Nitrous Oxide Emissions From Soils:

How Well Do We Understand the Processes and Their Controls?" *Philosophical Transactions of the Royal Society, B: Biological Sciences* 368, no. 1621: 20130122. https://doi.org/10.1098/rstb.2013.0122.

Butterbach-Bahl, K., G. Willibald, and H. Papen. 2002. "Soil Core Method for Direct Simultaneous Determination of N_2 and N_2O Emissions From Forest Soils." *Plant and Soil* 240, no. 1: 105–116. https://doi.org/10.1023/A:1015870518723.

Button, E. S., K. A. Marsden, P. D. Nightingale, et al. 2023. "Separating N_2O Production and Consumption in Intact Agricultural Soil Cores at Different Moisture Contents and Depths." *European Journal of Soil Science* 74, no. 2: e13363. https://doi.org/10.1111/ejss.13363.

Castellano-Hinojosa, A., N. Loick, E. Dixon, et al. 2019. "Improved Isotopic Model Based on ^{15}N Tracing and Rayleigh-Type Isotope Fractionation for Simulating Differential Sources of N_2O Emissions in a Clay Grassland Soil." *Rapid Communications in Mass Spectrometry* 33, no. 5: 449–460. https://doi.org/10.1002/rcm.8374.

Davidson, E. A., and S. Seitzinger. 2006. "The Enigma of Progress in Denitrification Research." *Ecological Applications* 16, no. 6: 2057–2063. https://doi.org/10.1890/1051-0761(2006)016[2057:TEOPID]2.0.CO;2.

Denmead, O. T., J. R. Freney, and J. R. Simpson. 1979. "Nitrous Oxide Emission During Denitrification in a Flooded Field." *Soil Science Society of America Journal* 43, no. 4: 716–718. https://doi.org/10.2136/sssaj1979.03615995004300040017x.

Ensign, S. H., M. F. Piehler, and M. W. Doyle. 2008. "Riparian Zone Denitrification Affects Nitrogen Flux Through a Tidal Freshwater River." *Biogeochemistry* 91, no. 2–3: 133–150. https://doi.org/10.1007/s10533-008-9265-9.

Escarmena, L., N. Roca, J. L. Riera, T. Sauras-Yera, S. Sabaté, and F. Sabater. 2024. "Impact of a WWTP Effluent Overland Flow on the Properties of a Mediterranean Riparian Soil." *Journal of Environmental Management* 366: 121778. https://doi.org/10.1016/j.jenvman.2024.121778.

Fisher, K., P. A. Jacinthe, P. Vidon, X. Liu, and M. E. Baker. 2014. "Nitrous Oxide Emission From Cropland and Adjacent Riparian Buffers in Contrasting Hydrogeomorphic Settings." *Journal of Environmental Quality* 43, no. 1: 338–348. https://doi.org/10.2134/jeq2013.06.0223.

Fowler, D., M. Coyle, U. Skiba, et al. 2013. "The Global Nitrogen Cycle in the Twenty-First Century." *Philosophical Transactions of the Royal Society, B: Biological Sciences* 368, no. 1621: 20130164. https://doi.org/10.1098/rstb.2013.0164.

Groh, T. A., M. P. Davis, T. M. Isenhart, D. B. Jaynes, and T. B. Parkin. 2019. "Denitrification Potential in Three Saturated Riparian Buffers." *Agriculture, Ecosystems & Environment* 286: 106656. https://doi.org/10.1016/j.agee.2019.106656.

Gu, C., W. Anderson, and F. Maggi. 2012. "Riparian Biogeochemical Hot Moments Induced by Stream Fluctuations." *Water Resources Research* 48, no. 9: 2011WR011720. https://doi.org/10.1029/2011WR011720.

Hallin, S., L. Philippot, F. E. Löffler, R. A. Sanford, and C. M. Jones. 2018. "Genomics and Ecology of Novel N_2O-Reducing Microorganisms." *Trends in Microbiology* 26, no. 1: 43–55. https://doi.org/10.1016/j.tim.2017.07.003.

Han, L., W. Huang, X. Yuan, Y. Zhao, Z. Ma, and J. Qin. 2017. "Denitrification Potential and Influencing Factors of the Riparian Zone Soils in Different Watersheds,Taihu Basin." *Water, Air, & Soil Pollution* 228, no. 3: 108. https://doi.org/10.1007/s11270-017-3287-7.

Harris, E., E. Diaz-Pines, E. Stoll, et al. 2021. "Denitrifying Pathways Dominate Nitrous Oxide Emissions From Managed Grassland During Drought and Rewetting." *Science Advances* 7, no. 6: eabb7118. https://doi.org/10.1126/sciadv.abb7118.

Hefting, M. M., R. Bobbink, and H. De Caluwe. 2003. "Nitrous Oxide Emission and Denitrification in Chronically Nitrate-Loaded Riparian Buffer Zones." *Journal of Environmental Quality* 32, no. 4: 1194–1203. https://doi.org/10.2134/jeq2003.1194.

Hefting, M. M., R. Bobbink, and M. P. Janssens. 2006. "Spatial Variation in Denitrification and N_2O Emission in Relation to Nitrate Removal Efficiency in a N-Stressed Riparian Buffer Zone." *Ecosystems* 9, no. 4: 550–563. https://doi.org/10.1007/s10021-006-0160-8.

Hu, H.-W., D. Chen, and J.-Z. He. 2015. "Microbial Regulation of Terrestrial Nitrous Oxide Formation: Understanding the Biological Pathways for Prediction of Emission Rates." *FEMS Microbiology Reviews* 39, no. 5: 729–749. https://doi.org/10.1093/femsre/fuv021.

IPCC. 2021. *Climate Change 2021—The Physical Science Basis: Working Group I Contribution to the Sixth Assessment Report of the Intergovernmental Panel on Climate Change*. 1st ed. Cambridge University Press. https://doi.org/10.1017/9781009157896.

Jacinthe, P.-A., and P. Vidon. 2017. "Hydro-Geomorphic Controls of Greenhouse Gas Fluxes in Riparian Buffers of the White River Watershed, IN (USA)." *Geoderma* 301: 30–41. https://doi.org/10.1016/j.geoderma.2017.04.007.

Jones, C. M., A. Spor, F. P. Brennan, et al. 2014. "Recently Identified Microbial Guild Mediates Soil N_2O Sink Capacity." *Nature Climate Change* 4, no. 9: 801–805. https://doi.org/10.1038/nclimate2301.

Kemmann, B., T. Ruf, A. Matson, and R. Well. 2023. "Waterlogging Effects on N_2O and N_2 Emissions From a Stagnosol Cultivated With Silphium Perfoliatum and Silage Maize." *Biology and Fertility of Soils* 59, no. 1: 53–71. https://doi.org/10.1007/s00374-022-01673-6.

Li, S., X. Xie, H. Li, and D. Xue. 2023. "Relationship Between Denitrification and Anammox Rates and N_2 Production With Substrate Consumption and pH in a Riparian Zone." *Environmental Technology* 45, no. 13: 1–10. https://doi.org/10.1080/09593330.2023.2177889.

Lind, L. P. D., J. Audet, K. Tonderski, and C. C. Hoffmann. 2013. "Nitrate Removal Capacity and Nitrous Oxide Production in Soil Profiles of Nitrogen Loaded Riparian Wetlands Inferred by Laboratory Microcosms." *Soil Biology and Biochemistry* 60: 156–164. https://doi.org/10.1016/j.soilbio.2013.01.021.

Liu, Y., L. Peng, H. H. Ngo, et al. 2016. "Evaluation of Nitrous Oxide Emission From Sulfide- and Sulfur-Based Autotrophic Denitrification Processes." *Environmental Science & Technology* 50, no. 17: 9407–9415. https://doi.org/10.1021/acs.est.6b02202.

Loick, N., E. Dixon, D. Abalos, et al. 2017. ""Hot Spots" of N and C Impact Nitric Oxide, Nitrous Oxide and Nitrogen Gas Emissions From a UK Grassland Soil." *Geoderma* 305: 336–345. https://doi.org/10.1016/j.geoderma.2017.06.007.

Maag, M., M. Malinovsky, and S. M. Nielsen. 1997. "Kinetics and Temperature Dependence of Potential Denitrification in Riparian Soils." *Journal of Environmental Quality* 26, no. 1: 215–223. https://doi.org/10.2134/jeq1997.00472425002600010031x.

Mafa-Attoye, T. G., M. A. Baskerville, E. Ofosu, M. Oelbermann, N. V. Thevathasan, and K. E. Dunfield. 2020. "Riparian Land-Use Systems Impact Soil Microbial Communities and Nitrous Oxide Emissions in an Agro-Ecosystem." *Science of the Total Environment* 724: 138148. https://doi.org/10.1016/j.scitotenv.2020.138148.

Mander, Ü., R. Well, D. Weymann, et al. 2014. "Isotopologue Ratios of N_2O and N2 Measurements Underpin the Importance of Denitrification in Differently N-Loaded Riparian Alder Forests." *Environmental Science & Technology* 48, no. 20: 11910–11918. https://doi.org/10.1021/es501727h.

Masta, M., M. Espenberg, S. S. Gadegaonkar, et al. 2022. "Integrated Isotope and Microbiome Analysis Indicates Dominance of Denitrification in N_2O Production After Rewetting of Drained Fen Peat." *Biogeochemistry* 161, no. 2: 119–136. https://doi.org/10.1007/s10533-022-00971-3.

Nadeem, S., P. Dörsch, and L. R. Bakken. 2013. "Autoxidation and Acetylene-Accelerated Oxidation of NO in a 2-Phase System: Implications for the Expression of Denitrification in Ex Situ

Experiments." *Soil Biology and Biochemistry* 57: 606–614. https://doi.org/10.1016/j.soilbio.2012.10.007.

Naiman, R. J., M. E. McClain, and H. Décamps. 2005. *Riparia: Ecology, Conservation, and Management of Streamside Communities*. Elsevier.

Nishisaka, C. S., C. Youngerman, L. K. Meredith, J. B. do Carmo, and A. A. Navarrete. 2019. "Differences in N_2O Fluxes and Denitrification Gene Abundance in the Wet and Dry Seasons Through Soil and Plant Residue Characteristics of Tropical Tree Crops." *Frontiers in Environmental Science* 7: 11. https://doi.org/10.3389/fenvs.2019.00011.

Petersen, R. J., Z. Liang, C. Prinds, et al. 2020. "Nitrate Reduction Pathways and Interactions With Iron in the Drainage Water Infiltration Zone of a Riparian Wetland Soil." *Biogeochemistry* 150, no. 2: 235–255. https://doi.org/10.1007/s10533-020-00695-2.

Sánchez-Pérez, J. M., C. Bouey, S. Sauvage, S. Teissier, I. Antiguedad, and P. Vervier. 2003. "A Standardised Method for Measuring In Situ Denitrification in Shallow Aquifers: Numerical Validation and Measurements in Riparian Wetlands." *Hydrology and Earth System Sciences* 7, no. 1: 87–96. https://doi.org/10.5194/hess-7-87-2003.

Seeberg-Elverfeldt, J., M. Schlüter, T. Feseker, and M. Kölling. 2005. "Rhizon Sampling of Porewaters Near the Sediment-Water Interface of Aquatic Systems." *Limnology and Oceanography: Methods* 3, no. 8: 361–371. https://doi.org/10.4319/lom.2005.3.361.

Vidon, P., and A. R. Hill. 2004. "Denitrification and Patterns of Electron Donors and Acceptors in Eight Riparian Zones With Contrasting Hydrogeology." *Biogeochemistry* 71, no. 2: 259–283. https://doi.org/10.1007/s10533-004-9684-1.

Vidon, P., S. Marchese, M. Welsh, and S. McMillan. 2015. "Short-Term Spatial and Temporal Variability in Greenhouse Gas Fluxes in Riparian Zones." *Environmental Monitoring and Assessment* 187, no. 8: 503. https://doi.org/10.1007/s10661-015-4717-x.

Vidon, P. G., M. K. Welsh, and Y. T. Hassanzadeh. 2018. "Twenty Years of Riparian Zone Research (1997–2017): Where to Next?" *Journal of Environmental Quality* 48, no. 2: 248–260. https://doi.org/10.2134/jeq2018.01.0009.

Walton, C. R., D. Zak, J. Audet, et al. 2020. "Wetland Buffer Zones for Nitrogen and Phosphorus Retention: Impacts of Soil Type, Hydrology and Vegetation." *Science of the Total Environment* 727: 138709. https://doi.org/10.1016/j.scitotenv.2020.138709.

Wang, F., K. D. Kroeger, M. E. Gonneea, J. W. Pohlman, and J. Tang. 2019. "Water Salinity and Inundation Control Soil Carbon Decomposition During Salt Marsh Restoration: An Incubation Experiment." *Ecology and Evolution* 9, no. 4: 1911–1921. https://doi.org/10.1002/ece3.4884.

Wang, R., G. Willibald, Q. Feng, et al. 2011. "Measurement of N_2, N_2O, NO, and CO_2 Emissions From Soil With the Gas-Flow-Soil-Core Technique." *Environmental Science & Technology* 45, no. 14: 6066–6072. https://doi.org/10.1021/es1036578.

Wang, S., Y. Pi, Y. Song, et al. 2020. "Hotspot of Dissimilatory Nitrate Reduction to Ammonium (DNRA) Process in Freshwater Sediments of Riparian Zones." *Water Research* 173: 115539. https://doi.org/10.1016/j.watres.2020.115539.

Welsh, M. K., P. G. Vidon, and S. K. McMillan. 2021. "Riparian Seasonal Water Quality and Greenhouse Gas Dynamics Following Stream Restoration." *Biogeochemistry* 156, no. 3: 453–474. https://doi.org/10.1007/s10533-021-00866-9.

Wild, J., M. Kopecký, M. Macek, M. Šanda, J. Jankovec, and T. Haase. 2019. "Climate at Ecologically Relevant Scales: A New Temperature and Soil Moisture Logger for Long-Term Microclimate Measurement." *Agricultural and Forest Meteorology* 268: 40–47. https://doi.org/10.1016/j.agrformet.2018.12.018.

Woodward, K. B., C. S. Fellows, C. L. Conway, and H. M. Hunter. 2009. "Nitrate Removal, Denitrification and Nitrous Oxide Production in the Riparian Zone of an Ephemeral Stream." *Soil Biology and Biochemistry* 41, no. 4: 671–680. https://doi.org/10.1016/j.soilbio.2009.01.002.

Wrage-Mönnig, N., M. A. Horn, R. Well, C. Müller, G. Velthof, and O. Oenema. 2018. "The Role of Nitrifier Denitrification in the Production of Nitrous Oxide Revisited." *Soil Biology and Biochemistry* 123: A3–A16. https://doi.org/10.1016/j.soilbio.2018.03.020.

Ye, F., L. Duan, Y. Sun, et al. 2023. "Nitrogen Removal in Freshwater Sediments of Riparian Zone: N-Loss Pathways and Environmental Controls." *Frontiers in Microbiology* 14: 1239055. https://doi.org/10.3389/fmicb.2023.1239055.

Zhang, L., Y. Liu, M. Jin, et al. 2023. "Influence of Seasonal Water-Level Fluctuations on Depth-Dependent Microbial Nitrogen Transformation and Greenhouse Gas Fluxes in the Riparian Zone." *Journal of Hydrology* 622: 129676. https://doi.org/10.1016/j.jhydrol.2023.129676.

Zheng, J., and P. V. Doskey. 2015. "Modeling Nitrous Oxide Production and Reduction in Soil Through Explicit Representation of Denitrification Enzyme Kinetics." *Environmental Science & Technology* 49, no. 4: 2132–2139. https://doi.org/10.1021/es504513v.

Supporting Information

Additional supporting information can be found online in the Supporting Information section.